

Ring finger protein 2 promotes colorectal cancer progression by suppressing early growth response 1

Feilong Wei^{1,*}, Haoren Jing^{2,*}, Ming Wei^{3,*}, Lei Liu⁴, Jieheng Wu⁵, Meng Wang⁵, Donghui Han⁶, Fa Yang⁶, Bo Yang⁶, Dian Jiao⁷, Guoxu Zheng⁵, Lingling Zhang⁵, Wenjin Xi⁵, Zhangyan Guo⁵, An-Gang Yang⁵, Weijun Qin⁶, Yi Zhou², Weihong Wen⁸

¹Department of Orthopedics, Tangdu Hospital, Fourth Military Medical University, Xi'an 710038, China

²Department of Anorectal Surgery, Tianjin Union Medical Center, Nankai University Affiliated Hospital, Tianjin 300013, China

³Urology Department of No. 989 Hospital, Joint Logistics Support Force of PLA, Luoyang 471000, China

⁴Department of Gastroenterology, Tangdu Hospital, Fourth Military Medical University, Xi'an 710038, China

⁵State Key Laboratory of Cancer Biology, Department of Immunology, Fourth Military Medical University, Xi'an 710032, China

⁶Department of Urology, Xijing Hospital, Fourth Military Medical University, Xi'an 710032, China

⁷Department of Urology, Tangdu Hospital, Fourth Military Medical University, Xi'an 710038, China

⁸Institute of Medical Research, Northwestern Polytechnical University, Xi'an 710072, China

*Equal contribution

Correspondence to: Weihong Wen, Yi Zhou, Weijun Qin; **email:** weihongwen@nwpu.edu.cn, zhouyi@umc.edu.cn, qinweij@fmmu.edu.cn

Keywords: RNF2, EGR1, colorectal cancer, cell proliferation, apoptosis

Received: November 25, 2019 **Accepted:** November 11, 2020 **Published:** December 19, 2020

Copyright: © 2020 Wei et al. This is an open access article distributed under the terms of the [Creative Commons Attribution License](https://creativecommons.org/licenses/by/3.0/) (CC BY 3.0), which permits unrestricted use, distribution, and reproduction in any medium, provided the original author and source are credited.

ABSTRACT

Ring finger protein 2 (RNF2) is an important component of polycomb repressive complex 1. RNF2 is upregulated in many kinds of tumors, and elevated RNF2 expression is associated with a poor prognosis in certain cancers. To assess the function of RNF2 in colorectal cancer, we examined RNF2 protein levels in 313 paired colorectal cancer tissues and adjacent normal tissues. We then analyzed the association of RNF2 expression with the patients' clinicopathologic features and prognoses. RNF2 expression was upregulated in colorectal cancer tissues and was associated with the tumor differentiation status, tumor stage and prognosis. In colorectal cancer cell lines, downregulation of RNF2 inhibited cell proliferation and induced apoptosis. Gene microarray analysis revealed that early growth response 1 (EGR1) was upregulated in RNF2-knockdown cells. Knocking down EGR1 partially reversed the inhibition of cell proliferation and the induction of apoptosis in RNF2-knockdown cells. RNF2 was enriched at the EGR1 promoter, where it mono-ubiquitinated histone H2A, thereby inhibiting EGR1 expression. These results indicate that RNF2 is oncogenic in colorectal cancer and may promote disease progression by inhibiting EGR1 expression. RNF2 is thus a potential prognostic marker and therapeutic target in colorectal cancer.

INTRODUCTION

Colorectal cancer (CRC) is among the most frequently diagnosed cancer types, with a worldwide incidence of >1,000,000 cases per year. Despite the

availability of treatments such as surgery, radiotherapy and chemotherapy, CRC is still a major contributor to cancer-associated mortality around the world [1]. Genetic and epigenetic mechanisms may promote the occurrence and progression of CRC

[2–4]. Thus, it is critical to further explore the pathways contributing to CRC occurrence and progression so that novel therapeutic targets and strategies can be determined.

Epigenetic regulation is one of the critical mechanisms that induce tumor occurrence and progression [5, 6]. The study of epigenetic regulators can not only reveal their function in tumor occurrence and progression, but also provide novel therapeutic targets. Indeed, as a result of functional studies of epigenetic regulators, the US Food and Drug Administration has approved inhibitors of DNA methyltransferases, histone deacetylases and Janus kinase 2 for particular cancer treatments [7–9].

Polycomb group (PcG) proteins are highly conserved epigenetic modifiers that function in multimeric complexes. In mammals, PcG proteins form two main complexes: polycomb repressive complexes 1 and 2 (PRC1 and PRC2). PRC1 is composed of BMI1, polyhomeotic, polycomb, Ring1a and ring finger protein 2 (RNF2, also known as Ring1b). PRC1 was shown to mono-ubiquitinate K119 of histone H2A [10–12]. PRC2 includes SUZ12, embryonic ectoderm development and enhancer of zeste 2, and was demonstrated to tri-methylate histone H3 at K27 [13, 14]. The modifications induced by PRC1 and PRC2 are transcriptionally repressive, and may influence each other [15]. PcG proteins participate in tumor occurrence and progression [16–18], and those that are oncogenic (such as enhancer of zeste 2 and BMI1) could be used as novel targets for cancer therapy [19–21].

RNF2 has been demonstrated to be the main PRC1 component that promotes H2A mono-ubiquitination at K119 [11]. RNF2 is upregulated in many human cancer types, and elevated RNF2 expression is an independent poor prognostic marker in pancreatic, breast, ovarian and bladder cancers [22–24]. In certain cancer types, RNF2 induces the ubiquitination/destabilization of p53 (directly or through MDM2), and the downregulation of RNF2 can suppress xenograft growth *in vivo* [25, 26]. Several genes have been identified as epigenetic targets of RNF2; for example, cyclin-dependent kinase inhibitors 1A and 2A (CDKN1A and CDKN2A) were shown to be RNF2 targets in hepatic stem/progenitor cells [27], and thioredoxin interacting protein was reported to be an RNF2 target in prostate cancer [28]. However, the involvement of RNF2 in CRC is unclear.

Here, we examined the expression of RNF2 in CRC tumor tissues and evaluated its association with clinicopathologic features and patients' prognoses. We also studied the function of RNF2 in CRC cell lines by

assessing the effects of downregulating RNF2 on cell proliferation and apoptosis. Finally, we explored the oncogenicity of RNF2 in terms of its effects on early growth response 1 (EGR1) expression. Our study indicated that RNF2 could be a novel prognostic marker and therapeutic target in CRC.

RESULTS

RNF2 was upregulated in CRC tissues

Immunohistochemistry was used to examine RNF2 expression in tissue microarrays containing 313 paired CRC tumor tissues and adjacent normal tissues. RNF2 protein levels were noticeably greater in CRC tumor tissues than in adjacent normal tissues (H-scores: 64.40 ± 56.14 and 43.54 ± 66.38 , respectively; Figure 1A, 1B). Patients were then separated into two groups based on their RNF2 levels, and were designated as RNF2-positive or RNF2-negative. When we analyzed the association between RNF2 levels and clinicopathologic characteristics, we observed that RNF2 positivity was associated with a significantly worse tumor differentiation status, tumor-node-metastasis (TNM) stage and Duke's stage (Table 1). These findings demonstrated that RNF2 expression is upregulated and significantly associated with the tumor differentiation status and tumor stage in CRC.

High RNF2 expression was associated with a poor prognosis in CRC patients

To determine the prognostic value of RNF2 in CRC, we assessed the relationship between RNF2 levels and overall survival. The overall survival time tended to be shorter in RNF2-positive patients than in RNF2-negative patients (Figure 1C). RNF2-positive patients also had shorter five-year local relapse-free survival and distant metastasis-free survival times than RNF2-negative patients (Figure 1D, 1E). In addition, the survival of patients with different tumor differentiation statuses, TNM stages and Duke's stages differed significantly between the RNF2-positive and RNF2-negative groups (Supplementary Figure 1A–1G).

Next, we performed a Cox regression analysis to determine the prognostic value of RNF2 in CRC patients. As shown in Table 2, in a univariate analysis, RNF2 expression, tumor cell differentiation, the Duke's stage and the TNM stage were all associated with the CRC prognosis. In a multivariate analysis, RNF2 positivity was associated with reduced overall survival, with an adjusted hazard ratio of 1.621 (95% confidence interval: 1.195–2.198; $p=0.002$). These results indicated that RNF2 can serve as an independent prognostic marker in CRC.

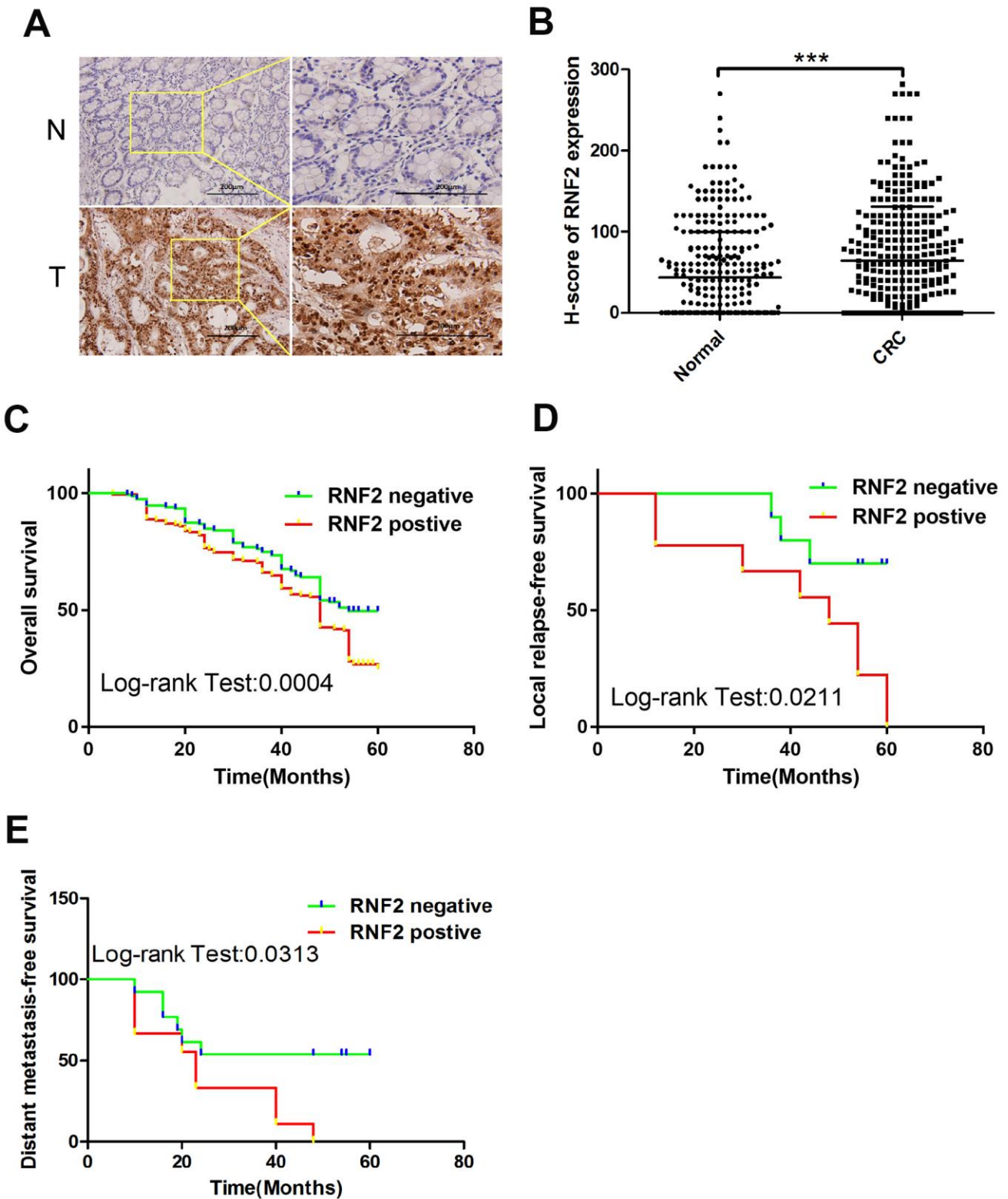


Figure 1. RNF2 expression was upregulated in CRC tumor tissues and was associated with patients' prognoses. (A) Representative immunohistochemistry results depicting positive and negative RNF2 staining in clinical CRC tumor tissues and adjacent normal tissues. The pictures on the right are the magnified view of the yellow boxes on the left. Scale bar: 200 μ m. **(B)** H-scores for RNF2 expression in 313 CRC tumor tissues and adjacent normal tissues. *** $p < 0.001$ versus adjacent normal tissue. **(C)** Overall survival of RNF2-positive or -negative CRC patients. **(D)** Local relapse-free survival of RNF2-positive or -negative CRC patients. **(E)** Distant metastasis-free survival of RNF2-positive or -negative CRC patients.

Table 1. The correlation between RNF2 expression and clinicopathological features in CRC patients (n=313).

Clinicopathological features	No. of patients (%)	RNF2 expression		χ^2	P value
		positive	negative		
Age (years)				0.007	0.932
≤ 60	128 (40.9%)	66	62		
> 60	185 (59.1%)	97	88		
Gender				0.135	0.713
Male	175 (55.9%)	94	81		
Female	138 (44.1%)	69	69		
Tumor invasion				7.933	0.088
T0	58 (18.5%)	48	10		
T1	35 (11.2%)	13	22		
T2	39 (12.5%)	21	18		
T3	176 (56.2%)	79	97		
T4	5 (1.6%)	2	3		
Lymph node metastasis				0.906	0.645
N0	226 (72.2%)	120	106		
N1	58 (18.5%)	32	26		
N2	29 (9.3%)	11	18		
Distant metastasis				1.183	0.277
M0	291 (93.0%)	154	137		
M1	22 (7.0%)	9	13		
Tumor differentiation				24.801	0.001*
Well	52 (16.6%)	21	31		
Moderately	155 (49.5%)	66	89		
Poorly	106 (33.9%)	76	30		
TNM stage				5.798	0.016*
I-II	213 (68.1%)	101	112		
III-IV	100 (31.9%)	62	38		
Dukes stage				5.632	0.018*
Dukes A-B	198 (63.3%)	93	105		
Dukes C-D	115 (36.7%)	70	45		

*Statistically significant (P < 0.05).

The downregulation of RNF2 reduced cell proliferation, promoted apoptosis and induced senescence in CRC cells

To study the function of RNF2 in CRC cells, we first assessed RNF2 levels in several CRC cell lines and a normal colon cell line (CRL-1459). RNF2 levels were obviously higher in all the CRC cells we examined than in normal colon cells (Supplementary Figure 2A). Then, we used short hairpin RNA (shRNA)-expressing lentiviruses to knock down RNF2 in HCT116 and WiDr cells, and confirmed the knockdown efficiency using Western blotting (Figure 2A, 2F). A 3-(4,5-dimethylthiazol-2-yl)-2,5-diphenyltetrazolium bromide (MTT) assay demonstrated that cell proliferation was dramatically inhibited in RNF2-knockdown HCT116 and WiDr cells (Figure 2B, 2D). To evaluate the effects of RNF2 downregulation on the survival of cells, we used flow cytometry to analyze apoptosis. The results indicated that knocking down RNF2 increased apoptosis in both HCT116 and WiDr cells, based on the increased

Annexin V⁺/propidium iodide⁻ cell percentages (Figure 2C, 2E). We also examined the cell cycle, and found that the proportion of cells in sub-G1 phase was greater in RNF2-knockdown cells than in control cells, further confirming that apoptosis was induced in RNF2-knockdown cells (Supplementary Figure 2B).

Next, we performed Western blotting, which revealed that both the mono-ubiquitination of H2A K119 and the expression of the cell cycle-related protein p21 were upregulated in RNF2-knockdown cells (Supplementary Figure 2C). We also used quantitative real-time PCR (qRT-PCR) and enzyme-linked immunosorbent assays (ELISAs) to analyze the mRNA and secreted protein levels of interleukin (IL)-6 and IL-8, which are markers of the senescence-associated secretory phenotype. Both the mRNA and secreted protein levels of IL-6 and IL-8 were upregulated in RNF2-knockdown HCT116 cells (Figure 2G, 2H). These results indicated that RNF2 promotes cell proliferation and inhibits apoptosis and senescence in CRC cells.

Table 2. Cox regression analysis of prognostic factors for overall survival in CRC patients (n=313).

	Univariate			Multivariate		
	HR	95% CI	P value	HR	95% CI	P value
RNF2 expression (Negative vs. Positive)	1.635	1.225-2.181	0.001*	1.621	1.195-2.198	0.002*
Age (> 60 vs. ≤ 60)	1.133	0.849-1.512	0.397	1.119	0.831-1.507	0.459
Gender (Female vs. Male)	1.070	0.807-1.419	0.638	0.966	0.721-1.295	0.817
TNM stage			0.002*			0.001*
TNM2 vs. TNM1	0.628	0.436-0.905	0.013	0.464	0.305-0.707	0.001
TNM3 vs. TNM1	0.715	0.461-1.109	0.134	0.355	0.203-0.620	0.001
TNM4 vs. TNM1	1.326	0.829-2.121	0.239	0.859	0.509-1.449	0.568
Differentiation			0.027*			0.011*
Moderately vs. well	0.771	0.569-1.044	0.092	0.914	0.665-1.257	0.581
Poorly vs. well	0.556	0.356-0.868	0.010	0.485	0.300-0.783	0.003
Dukes stage			0.010*			0.031*
Dukes B vs. Dukes A	0.743	0.480-1.153	0.185	0.889	0.545-1.449	0.637
Dukes C vs. Dukes A	1.033	0.660-1.618	0.886	1.365	0.800-2.331	0.254
Dukes D vs. Dukes A	2.037	0.982-4.227	0.056	2.175	0.972-4.866	0.059

Abbreviations: HR, hazard ratio; 95% CI, 95% confidence interval.

*Statistically significant ($P < 0.05$).

The downregulation of RNF2 induced EGR1 expression

To investigate the molecular pathways through which RNF2 induced cell proliferation and suppressed apoptosis and senescence in CRC, we conducted a gene microarray analysis using mRNAs from RNF2-knockdown and control HCT116 cells. When a 1.5-fold difference in expression was used as the cutoff, 544 genes were differentially expressed between RNF2-knockdown cells and control cells, with 135 being upregulated and 409 being downregulated in RNF2-knockdown cells. These differentially expressed genes were evaluated using Gene Ontology and Kyoto Encyclopedia of Genes and Genomes analyses (Supplementary Figure 3A–3D). Some of the most significantly changed genes that are involved in cell proliferation and apoptosis are shown in Figure 3A.

Since PcG proteins transcriptionally repress gene expression, we concentrated on several tumor suppressors that were upregulated in RNF2-knockdown cells. EGR1 expression was significantly upregulated in RNF2-knockdown HCT116 and WiDr cells. In RNF2-knockdown HCT116 cells, the mRNA and protein levels of RNF2 decreased gradually over time after the lentiviral infection, while the mRNA and protein levels of EGR1 gradually increased (Figure 3B, 3C and Supplementary Figure 4A, 4B).

Then, we analyzed EGR1 expression and its correlation with RNF2 expression in CRC tissues. Among the 313 CRC tissues, 52.1% (163/313) were RNF2-positive, while

56.7% were EGR1-negative (178/313). A correlation analysis indicated that RNF2 expression correlated negatively with EGR1 expression in CRC tissues ($r = -0.12$; Supplementary Figure 5A, 5B). These results indicated that RNF2 may downregulate EGR1 in CRC.

Knocking down EGR1 partially reversed the inhibition of cell proliferation and the increase in apoptosis in RNF2-knockdown cells

To determine whether EGR1 is a downstream target of RNF2, we performed rescue experiments by simultaneously knocking down EGR1 and RNF2 in HCT116 cells. Western blotting confirmed the knock-down efficiency (Figure 4A). An MTT assay demonstrated that knocking down EGR1 partially reversed the inhibition of cell proliferation in RNF2-knockdown cells (Figure 4B). Flow cytometry indicated that knocking down EGR1 partially reversed the increase in apoptosis in RNF2-knockdown cells (Figure 4C). Poly(ADP-ribose) polymerase (PARP) cleavage was also reduced in the EGR1/RNF2 double-knockdown cells, further demonstrating the partial inhibition of apoptosis (Figure 4A). These findings demonstrated that RNF2 promotes cell proliferation and inhibits apoptosis by downregulating EGR1 in CRC cells.

The downregulation of RNF2 reduced both RNF2 enrichment and H2A mono-ubiquitination at the EGR1 promoter

To assess whether RNF2 directly inhibits EGR1 expression, we performed chromatin immunoprecipitation

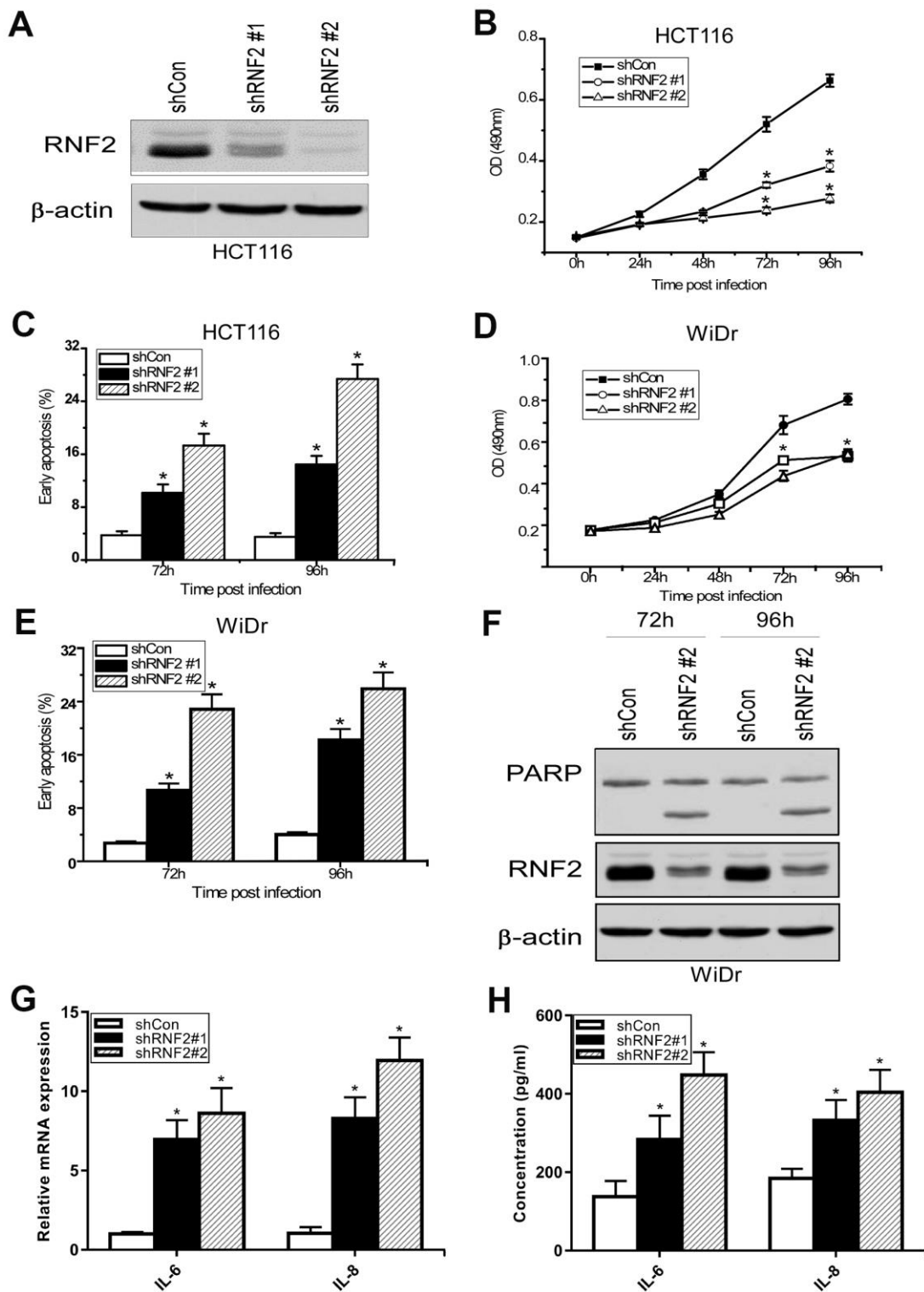


Figure 2. The downregulation of RNF2 inhibited cell proliferation and increased apoptosis in CRC cells. (A) Western blot analysis showing the knockdown efficiency of RNF2 in HCT116 cells that had been infected with shRNA-expressing lentiviruses for 48 hours. (B) MTT assay showing the proliferation of RNF2-knockdown and control HCT116 cells. (C) Apoptosis analysis of RNF2-knockdown and control HCT116 cells. (D) MTT assay showing the proliferation of RNF2-knockdown and control WiDr cells. (E) Apoptosis analysis of RNF2-knockdown and control WiDr cells. (F) Western blot analysis showing the knockdown efficiency of RNF2 and the cleavage of PARP in RNF2-knockdown and control WiDr cells. (G) qRT-PCR analysis showing the mRNA levels of IL-6 and IL-8 in RNF2-knockdown and control HCT116 cells. (H) ELISA assay showing the soluble IL-6 and IL-8 levels in culture media. Three independent experiments were performed and analyzed for B-E. Data represent the mean \pm standard deviation. * $p < 0.05$ versus shCon group.

(ChIP) assays using antibodies against RNF2 and mono-ubiquitinated H2A K119 (H2A K119Ub). We designed three primer pairs to amplify specific regions up to 2000 base pairs upstream of the transcription start site of EGR1 (Figure 5A). We found that RNF2 and mono-ubiquitinated H2A were specifically enriched in the same region of the EGR1 promoter (Figure 5B). We also

performed ChIP assays in control and RNF2-knockdown HCT116 cells, and observed that both RNF2 enrichment and H2A mono-ubiquitination at the EGR1 promoter were inhibited in RNF2-knockdown cells (Figure 5C). These findings demonstrated that RNF2 binds directly to the EGR1 promoter, where it mono-ubiquitinates H2A, thus inhibiting EGR1 expression.

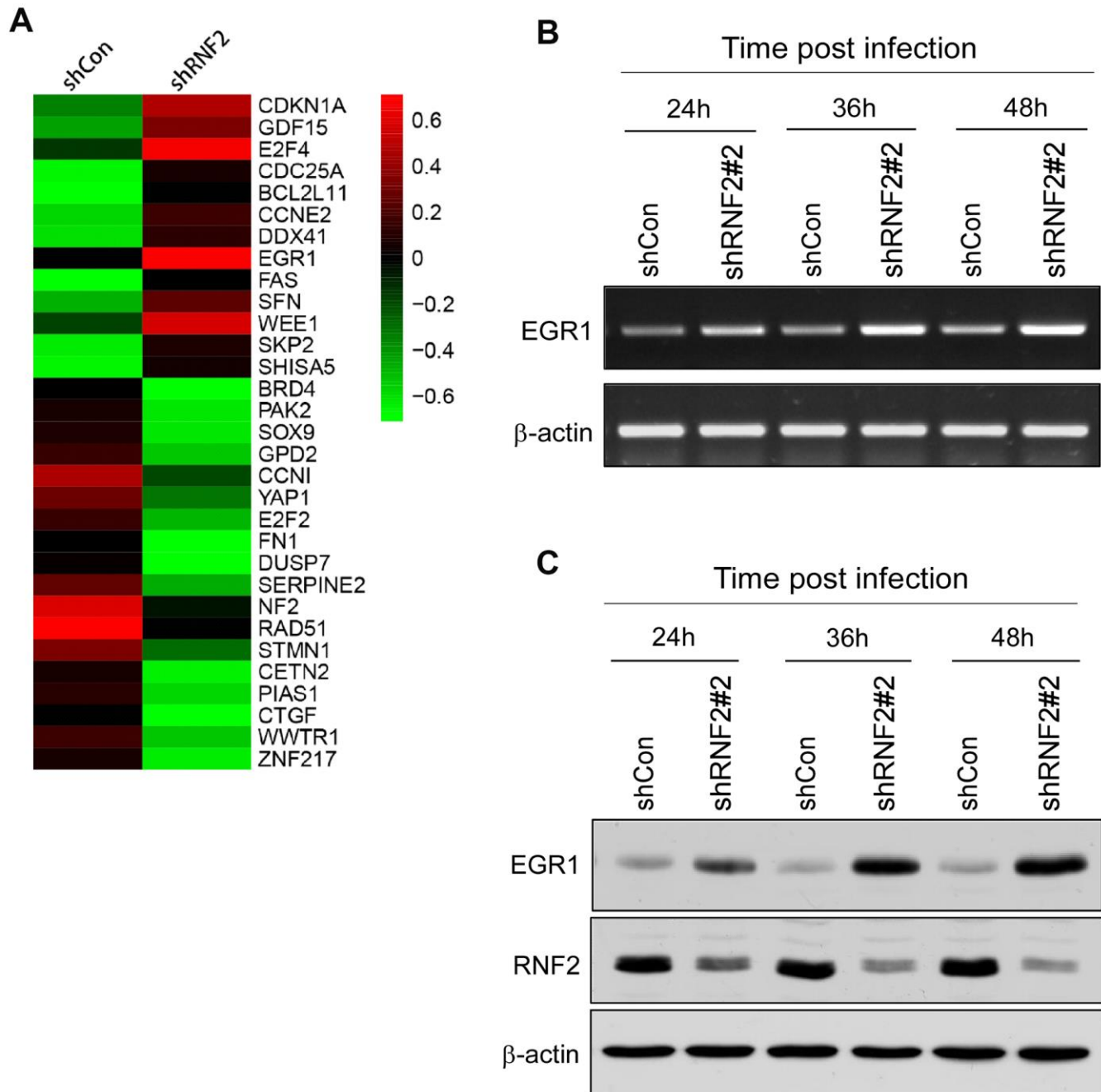


Figure 3. The downregulation of RNF2 induced EGR1 expression. (A) Heat map of some of the most differentially expressed genes in shRNF2-treated HCT116 cells, determined through microarray analyses (red: upregulated; green: downregulated). (B) RT-PCR analysis showing the increased EGR1 mRNA levels in RNF2-knockdown HCT116 cells. (C) Western blot showing the increased EGR1 protein levels in RNF2-knockdown HCT116 cells.

DISCUSSION

Epigenetic modifications such as DNA methylation, histone modification and small non-coding RNA regulation are all major contributors to tumor occurrence and progression [5, 6]. PcG proteins are important epigenetic regulators that repress transcription mainly by modifying histones, and several of these proteins are upregulated in and involved in the progression of numerous cancer types. Several studies have demonstrated that the expression of RNF2, a PcG protein, is associated with the tumor grade and prognosis, and

could serve as a prognostic biomarker and therapeutic target in certain cancer types [22–24, 29, 30]. However, the function of RNF2 in CRC has not been determined.

We first evaluated RNF2 expression in 313 paired CRC tumor tissues and adjacent normal tissues, and observed that RNF2 was markedly upregulated in CRC tumor tissues. RNF2 expression was associated with clinicopathologic features such as the tumor differentiation status, TNM stage and Duke's stage. In addition, RNF2 expression was associated with patients' prognoses, as the survival times tended to be

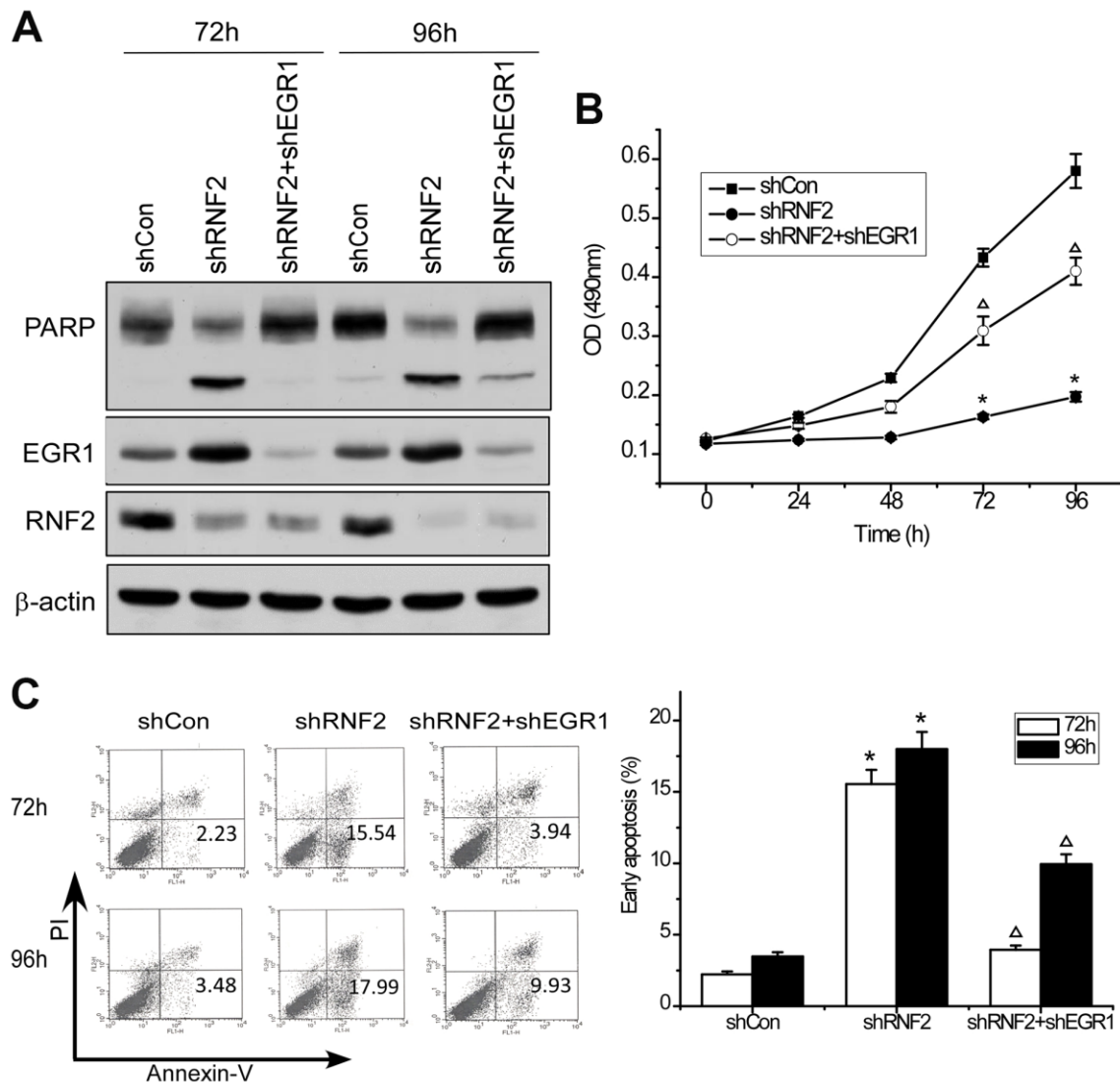


Figure 4. Knocking down EGR1 partially reversed the inhibition of cell proliferation and the increase in apoptosis in RNF2-knockdown cells. (A) Western blot showing the knockdown efficiency of RNF2 and EGR1 and the cleavage of PARP in RNF2/EGR1 double-knockdown, RNF2-knockdown and control HCT116 cells. (B) MTT assay showing the proliferation of RNF2/EGR1 double-knockdown, RNF2-knockdown and control HCT116 cells. (C) Apoptosis analysis of RNF2/EGR1 double-knockdown, RNF2-knockdown and control HCT116 cells. Three independent experiments were performed and analyzed for B and C. Data represent the mean \pm standard deviation. * $p < 0.05$ versus shCon, $^{\Delta}p < 0.05$ versus shRNF2.

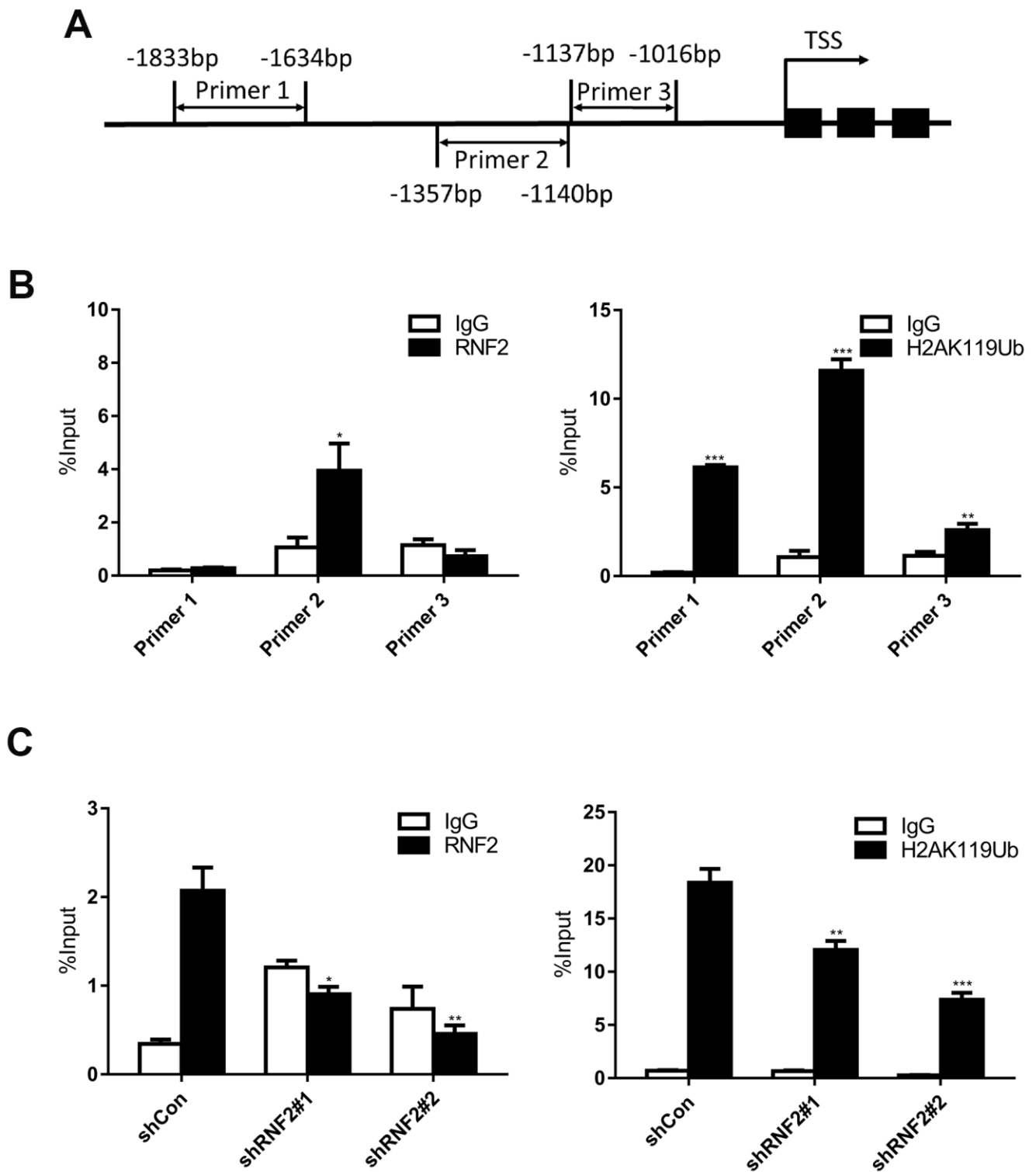


Figure 5. The downregulation of RNF2 reduced both RNF2 enrichment and H2A mono-ubiquitination at the EGR1 promoter. (A) The positions of the three PCR primer sets used in the ChIP assay. (B) Quantitative PCR analysis after a ChIP assay using antibodies against RNF2 and H2A K119Ub. Three independent experiments were performed and analyzed. Data represent the mean \pm standard deviation. * $p < 0.05$, ** $p < 0.01$ and *** $p < 0.001$ versus IgG. (C) Quantitative PCR analysis using primer set 2 after a ChIP assay to show the enrichment of RNF2 and the mono-ubiquitination of H2A at the EGR1 promoter in RNF2-knockdown and control HCT116 cells. Three independent experiments were performed and analyzed. Data represent the mean \pm standard deviation. * $p < 0.05$, ** $p < 0.01$ and *** $p < 0.001$ versus shCon.

shorter in RNF2-positive patients than in RNF2-negative patients. We also studied RNF2 function by using shRNA to knock down RNF2 in CRC cells, and observed that the downregulation of RNF2 inhibited cell proliferation, promoted apoptosis and induced senescence in CRC cells.

We then performed a gene microarray analysis to identify the molecular pathways through which RNF2 altered CRC cell proliferation, apoptosis and senescence. In total, 554 genes exhibited an expression difference of at least 1.5-fold between RNF2-knockdown cells and control cells. Considering that PcG proteins repress gene transcription, we mostly concentrated on tumor suppressors that were upregulated in RNF2-knockdown cells. EGR1 expression was clearly upregulated in RNF2-knockdown HCT116 and WiDr cells; thus, we further explored whether EGR1 was a target of RNF2.

EGR1 is a transcription factor in the immediate-early gene group, and alters the expression of various genes involved in development, cellular differentiation and proliferation [31–33]. EGR1-knockout mice exhibit accelerated tumor development, and p53 has been identified as a direct target of EGR1 [34, 35]. Several other tumor suppressors are also targets of EGR1, including transforming growth factor- β , phosphatase and tensin homolog, p73 and fibronectin [36]. EGR1, p53 and p73 have been found to network to induce apoptosis in tumor cells [37]. EGR1 also binds to the promoter of CDKN2B and the first intron of CDKN1A to upregulate their expression and stimulate RAF-induced senescence [38].

Because it upregulates several tumor suppressor genes, EGR1 is also considered to be a tumor suppressor, and lower EGR1 expression has been associated with poorer outcomes in many cancer types, including non-small-cell lung cancer, osteosarcoma, glioma and breast cancer [39–42]. However, some studies have indicated that EGR1 may accelerate tumor progression by stimulating cellular proliferation, invasion and angiogenesis in certain cancer types, such as prostate, ovarian, gastric and liver cancers [43–47]. In CRC, EGR1 has been found to promote or suppress tumor growth, depending on the cell type and environment. For example, Kim et al. reported that EGR1 overexpression promoted the growth of LS174T cells, indicating that EGR1 has an oncogenic function [48]. However, Lee et al. demonstrated that EGR1 overexpression stimulated apoptosis, while EGR1 silencing prevented apoptosis in tolfenamic acid-treated CRC cells [49]. Han et al. found that sanguinarine markedly induced EGR1 expression, while knocking down EGR1 significantly

inhibited sanguinarine-induced apoptosis in HCT116 cells [50]. In addition, Choi et al. found that 26.6% of CRC patients carried EGR1 frameshift mutations and mutational intratumoral heterogeneities [51]. Thus, several studies have indicated that EGR1 is a tumor suppressor in CRC.

In the present study, we found that EGR1 mRNA and protein levels were elevated in RNF2-knockdown CRC cells. Knocking down EGR1 partially reversed the inhibition of proliferation and the increase in apoptosis in RNF2-knockdown cells, confirming that EGR1 is a downstream target of RNF2. We also examined RNF2 and EGR1 levels in clinical CRC tissues, and detected a negative correlation between them. We then used ChIP assays to determine the mechanism whereby RNF2 suppressed EGR1 expression, and found that RNF2 was enriched at the EGR1 promoter. In RNF2-knockdown cells, both RNF2 enrichment and H2A mono-ubiquitination at the EGR1 promoter decreased, indicating that RNF2 downregulates EGR1 by mono-ubiquitinating H2A.

However, knocking down EGR1 did not completely reverse the inhibition of cell proliferation and the increase in apoptosis in RNF2-knockdown cells, indicating that RNF2 may also function through other mechanisms. For example, p21 was also upregulated in RNF2-knockdown HCT116 cells, suggesting that p21 may be a downstream target of RNF2 in CRC, consistent with a previous study in hepatic stem/progenitor cells [27]. Since EGR1 has been demonstrated to upregulate CDKN1A [38], the increase in p21 expression may have been induced by the increase in EGR1 expression in RNF2-knockdown cells. Our gene microarray analysis also revealed other genes that may be targets of RNF2, so these genes deserve further evaluation.

EGR1 expression is regulated by several transcription factors, including ETS and activating transcription factor 3 [49, 52]. EGR1 expression can also be altered by different epigenetic modifications, such as histone acetylation, methylation and ubiquitination [53–55]. Further evaluation is needed to determine whether there is a correlation between transcription factor-induced regulation and epigenetic regulation. Recently, a PRC1-specific inhibitor, PRT4165 (2-pyridine-3-yl-methyleneindan-1,3-dione), was found to suppress RNF2-induced H2A ubiquitination, thus inhibiting DNA repair following DNA damage [56]. Considering our finding that downregulating RNF2 inhibited cell growth and induced apoptosis in CRC cells, further investigation is warranted to assess whether PRT4165 can inhibit cell growth, induce apoptosis and be applied in the treatment of CRC.

In summary, our study revealed that RNF2 expression was greater in CRC tumor tissues than in adjacent normal tissues, and was associated with the clinicopathologic features and prognoses of CRC patients. We demonstrated that RNF2 may exert its oncogenic functions by transcriptionally repressing EGR1 in CRC. Thus, RNF2 could be used as a novel prognostic biomarker and therapeutic target in CRC.

MATERIALS AND METHODS

Patients and follow-up

This study was approved by the ethics committee of the Fourth Military Medical University. All the involved patients gave their written informed consent. The CRC tissue microarrays contained 313 CRC tumor tissues and paired adjacent normal tissues that were collected from patients at the Department of Anorectal Surgery, Tianjin Union Medical Center, from February 2004 to December 2005. None of the patients were treated with chemotherapy or radiotherapy before surgery, and all of them received chemotherapy after surgery. The criteria of the Union for International Cancer Control were used to classify the histology and clinical stage of each patient. Each participant's follow-up information was updated every four months through phone calls. The overall survival time was defined from the date of surgery to death. The deaths of patients were confirmed by their families.

Immunohistochemistry

Immunohistochemistry was used to examine RNF2 expression in paraffin-embedded tissue microarray sections containing 313 CRC tumor tissues and adjacent normal colon tissues. In brief, the slides were deparaffinized in xylene and rehydrated using a graded alcohol series. Then, 3% H₂O₂ was used to block endogenous peroxidase activity, and pre-immune rabbit serum was used to block non-specific protein binding. The slides were then incubated with an anti-RNF2 antibody (Abcam, ab101273) overnight in a humidified chamber at 4° C. Subsequently, the slides were washed with phosphate-buffered saline (PBS) and incubated with a horseradish peroxidase-conjugated secondary antibody for 30 minutes at room temperature. Then, the slides were incubated with 3, 3'-diaminobenzidine chromogen for 2-3 minutes for visualization. The slides were counterstained with hematoxylin, and RNF2 expression was evaluated using the H-score method by two pathologists who were blinded to the patients' clinical information [19]. The H-score was calculated as the sum of the cells with strong signals (3×), moderate signals (2×) and weak signals (1×) in one hundred cells. The H-scores ranged from 0 to 300, and patients with

H-scores higher than 50 were designated as RNF2-positive, while those with H-scores lower than 50 were designated as RNF2-negative.

Cell culture

Human colon cancer cells (HCT116 and WiDr) were obtained from the Type Culture Collection of the Chinese Academy of Sciences (Shanghai, China). The cells were cultured in McCoy's 5A medium (HCT116) or Eagle's minimum essential medium (WiDr) supplemented with 10% fetal bovine serum and 1% penicillin-streptomycin in a humidified incubator containing 5% CO₂ at 37° C.

Lentiviral packaging and cell infection

Lentiviral plasmids expressing shRNA against RNF2 (shRNF2 #1, #2) were purchased from Open Biosystems (Huntsville, AL, USA). Lipofectamine 2000 (Invitrogen, Carlsbad, CA, USA) or JetPEI (Polyplus Transfection, New York, NY, USA) was used to transfect cells with the plasmid DNA. For virus packaging, the shRNF2-containing lentiviral plasmids were co-transfected with packaging and envelope plasmids (psPAX.2 and pMD2.G) into 293T cells. The lentiviruses were collected 36 and 60 hours after transfection, and were centrifuged at 1000 rpm for 5 minutes before the supernatants were harvested. HCT116 and WiDr cells were infected with the lentiviruses, together with 8 µg/mL polybrene (Millipore, Billerica, MA, USA).

RT-PCR

Total RNA was extracted with an RNeasy Plus Universal Mini Kit (QIAGEN, Hilden, Germany). The quantity and quality of the RNA were examined with a NanoDrop 2000 (Thermo Scientific, USA). The RNA was reverse-transcribed into cDNA using a Revert AidTM First Strand cDNA Synthesis Kit (Fermentas, St. Leon-Rot, Germany), and used as a template. The PCR primer sequences were as follows: EGR1, Forward: 5'-CTGACCAGAGTCTTTTCCTG-3', Reverse: 5'-CTGACCGCAGAGTCTTTTCCTG-3'; β-actin, Forward: 5'-CCGTGTGAACCATGTGACTT-3', Reverse: 5'-CTAAGTTCCTCCTA-3'.

Western blot

Radioimmunoprecipitation assay lysis buffer supplemented with a protease inhibitor cocktail (Roche, Indianapolis, IN, USA) was used for cell lysate extraction. The protein concentration was determined using a bicinchoninic acid assay. The proteins from the cell lysates were electrophoretically separated on 10%

sodium dodecyl sulfate polyacrylamide gels and transferred onto nitrocellulose membranes (Millipore, Bedford, MA, USA). The membranes were blocked in 5% nonfat milk for 1 hour at room temperature before they were incubated with primary antibodies overnight at 4° C. The antibodies used in this study included anti-RNF2 antibody (CST, #5694), anti-EGR1 antibody (CST, #4153) and anti-β-actin antibody (Sigma, A5441). The membranes were then washed three times with Tris-buffered saline-Tween and incubated with a horseradish peroxidase-conjugated secondary antibody for 1 hour at room temperature. Protein bands were visualized and photographed using a FluorChem FC2 system (Alpha Innotech, San Leandro, CA, USA).

MTT assay

An MTT assay was used to assess *in vitro* cell proliferation. Cells that had been infected with lentiviruses (control [shCon], shRNF2 and/or shEGR1) for 24 hours were plated on 96-well plates at a density of 3×10^4 cells/mL, 100 μL per well. At the timepoint of examination, each well was treated with 20 μL of MTT substrate (from a 2.5 mg/mL stock solution in PBS), and the plates were placed in an incubator for 4 hours. Then, the culture medium was replaced with 150 μL of dimethylsulfoxide, and the plates were gently shaken for 15 minutes before the absorbance at 492 nm was obtained using a spectrophotometer. The plates were analyzed at the indicated timepoints for five consecutive days.

Apoptosis and cell cycle analysis

HCT116 or WiDr cells were infected with shRNA lentiviruses (shCon, shRNF2 and/or shEGR1) for 72 or 96 hours before analysis. For the analysis of apoptosis, the cells were trypsinized, counted and suspended in PBS (1×10^6 cells per group). Then, the cells were incubated with Annexin V-fluorescein isothiocyanate and propidium iodide (BD Biosciences, CA, USA) for 15 minutes in the dark at room temperature. Apoptotic cells were then assessed on a flow cytometer (CYTOMICS FC 500, Beckman Coulter). For the analysis of the cell cycle, cells were harvested, washed with ice-cold PBS and fixed with 70% ice-cold ethanol. Then, the cells were centrifuged, resuspended in PBS containing RNase (100 μg/mL) and propidium iodide (40 μg/mL), and incubated at 37° C for 1 hour. The cell cycle was then analyzed using flow cytometry.

ELISA

ELISA assays were used to evaluate the secreted protein levels of IL-6 and IL-8 in culture media from control and RNF2-knockdown cells. ELISA kits for human

IL-6 and IL-8 were used in accordance with the manufacturer's manual (CUSABIO BIOTEC Co., Ltd, Wuhan, China).

Gene microarray analysis

Total RNA was extracted from HCT116 cells that had been infected with shCon or shRNF2 #2 for 48 hours. The RNA was then quantified and sent to Phalanx Biotech Group for gene expression analysis using a Human Whole Genome OneArray™ (HOAv4.3, Phalanx Biotech Group, Taiwan). The RNA was amplified and hybridized with 10 μg of fragmented biotin-labeled complementary RNA at 50° C for 14-16 hours in triplicate. Then, non-specific binding targets were removed, and the hybridization arrays were conjugated with a Streptavidin-Cy3-labeled detector. The arrays were then dried and scanned on a DNA Microarray Scanner, and the data were quantified and analyzed.

ChIP assay

The ChIP assay was conducted according to a previously published method, with slight modifications [28]. Briefly, HCT116 cells in the different groups were treated with 1% formaldehyde for 15 minutes at room temperature to cross-link proteins and DNA. The cells were then harvested, centrifuged and resuspended in radio-immunoprecipitation assay buffer containing a protease inhibitor cocktail. The cell lysates were sonicated to ensure that the chromatin was sheared to a length of 200-1000 base pairs on average. The sheared chromatin was then subjected to immunoprecipitation with different antibodies, including an anti-RNF2 antibody (CST, #5694), anti-H2A K119Ub antibody (CST, #8240) and control IgG (isotype control) (CST, #2729) with magnetic beads. The immunoprecipitants were eluted and reverse cross-linked, and the proteins were digested with proteinase K. The purified DNA was then used for RT-PCR. The primers used in this study were designed according to the sequence upstream of the transcription start site of EGR1. The primers were: Primer set 1, Forward: 5'-GGACAGCCACAGAGGGATTA-3', Reverse: 5'-TCCAGAGGAGGTGCTGTTTT-3'; Primer set 2, Forward: 5'-CTGCTCAGTTCGTGCTCACT-3', Reverse: 5'-GCTTCCCTATGGGCTGTCTG-3'; Primer set 3, Forward: 5'-CTCTTTCGGATTCCCGCAGT-3', Reverse: 5'-CCCCAAGAGAGGCCTGATTC-3'.

Statistical analysis

Statistical analyses were performed using IBM SPSS statistical software (version 20.0). Student's t test was used for data analysis. Survival curves were generated using the Kaplan-Meier method, and distributions were

compared using the log-rank test. The hazard ratios for factors associated with survival were determined using Cox proportional hazard models. Differences between two groups were analyzed using χ^2 tests and Fisher's exact tests. Correlations were assessed with Spearman's correlation analysis. P values < 0.05 were considered to be statistically significant.

AUTHOR CONTRIBUTIONS

Weihong Wen, Yi Zhou and Weijun Qin designed the experiments. Feilong Wei, Haoren Jing and Ming Wei conducted the experiments, analyzed the results and wrote the article. Lei Liu, Jieheng Wu and Meng Wang helped to analyze the results and revise the figures. Donghui Han, Fa Yang, Bo Yang, Dian Jiao, Guoxu Zheng, Lingling Zhang, Wenjin Xi and Zhangyan Guo conducted some of the experiments. Weihong Wen, Yi Zhou, Weijun Qin and An-Gang Yang assisted in the analysis of the results and the revision the manuscript.

ACKNOWLEDGMENTS

We thank Dr. Yi Wan (Department of Health Services, School of Public Health, Fourth Military Medical University, China) for help with the statistical analysis. We thank Mrs. Yunxin Cao and Mr. Jintao Hu (Department of Immunology, Fourth Military Medical University, China) for the flow cytometry analysis.

CONFLICTS OF INTEREST

The authors declare that they have no conflicts of interest.

FUNDING

This study was supported by the National Natural Science Foundation of China (No. 81372225, 81372771, 81772734 and 81171924), and the MOST Special Fund from the State Key Laboratory of Cancer Biology (Fourth Military Medical University) (CBSKL2014Z16).

REFERENCES

1. Siegel RL, Miller KD, Jemal A. Cancer statistics, 2019. *CA Cancer J Clin.* 2019; 69:7–34. <https://doi.org/10.3322/caac.21551> PMID:[30620402](https://pubmed.ncbi.nlm.nih.gov/30620402/)
2. Migliore L, Migheli F, Spisni R, Coppedè F. Genetics, cytogenetics, and epigenetics of colorectal cancer. *J Biomed Biotechnol.* 2011; 2011:792362. <https://doi.org/10.1155/2011/792362> PMID:[21490705](https://pubmed.ncbi.nlm.nih.gov/21490705/)
3. Toyota M, Suzuki H, Yamamoto E, Yamano H, Imai K, Shinomura Y. Integrated analysis of genetic and epigenetic alterations in cancer. *Epigenomics.* 2009; 1:291–99. <https://doi.org/10.2217/epi.09.20> PMID:[22122704](https://pubmed.ncbi.nlm.nih.gov/22122704/)
4. Pino MS, Chung DC. The chromosomal instability pathway in colon cancer. *Gastroenterology.* 2010; 138:2059–72. <https://doi.org/10.1053/j.gastro.2009.12.065> PMID:[20420946](https://pubmed.ncbi.nlm.nih.gov/20420946/)
5. Rodríguez-Paredes M, Esteller M. Cancer epigenetics reaches mainstream oncology. *Nat Med.* 2011; 17:330–39. <https://doi.org/10.1038/nm.2305> PMID:[21386836](https://pubmed.ncbi.nlm.nih.gov/21386836/)
6. Portela A, Esteller M. Epigenetic modifications and human disease. *Nat Biotechnol.* 2010; 28:1057–68. <https://doi.org/10.1038/nbt.1685> PMID:[20944598](https://pubmed.ncbi.nlm.nih.gov/20944598/)
7. Dawson MA, Kouzarides T. Cancer epigenetics: from mechanism to therapy. *Cell.* 2012; 150:12–27. <https://doi.org/10.1016/j.cell.2012.06.013> PMID:[22770212](https://pubmed.ncbi.nlm.nih.gov/22770212/)
8. Helin K, Dhanak D. Chromatin proteins and modifications as drug targets. *Nature.* 2013; 502:480–88. <https://doi.org/10.1038/nature12751> PMID:[24153301](https://pubmed.ncbi.nlm.nih.gov/24153301/)
9. Kelly TK, De Carvalho DD, Jones PA. Epigenetic modifications as therapeutic targets. *Nat Biotechnol.* 2010; 28:1069–78. <https://doi.org/10.1038/nbt.1678> PMID:[20944599](https://pubmed.ncbi.nlm.nih.gov/20944599/)
10. Vidal M. Role of polycomb proteins Ring1A and Ring1B in the epigenetic regulation of gene expression. *Int J Dev Biol.* 2009; 53:355–70. <https://doi.org/10.1387/ijdb.082690mv> PMID:[19412891](https://pubmed.ncbi.nlm.nih.gov/19412891/)
11. Wang H, Wang L, Erdjument-Bromage H, Vidal M, Tempst P, Jones RS, Zhang Y. Role of histone H2A ubiquitination in polycomb silencing. *Nature.* 2004; 431:873–78. <https://doi.org/10.1038/nature02985> PMID:[15386022](https://pubmed.ncbi.nlm.nih.gov/15386022/)
12. Levine SS, Weiss A, Erdjument-Bromage H, Shao Z, Tempst P, Kingston RE. The core of the polycomb repressive complex is compositionally and functionally conserved in flies and humans. *Mol Cell Biol.* 2002; 22:6070–78. <https://doi.org/10.1128/mcb.22.17.6070-6078.2002> PMID:[12167701](https://pubmed.ncbi.nlm.nih.gov/12167701/)
13. Kuzmichev A, Nishioka K, Erdjument-Bromage H, Tempst P, Reinberg D. Histone methyltransferase activity associated with a human multiprotein complex containing the Enhancer of Zeste protein. *Genes Dev.* 2002; 16:2893–905. <https://doi.org/10.1101/gad.1035902> PMID:[12435631](https://pubmed.ncbi.nlm.nih.gov/12435631/)

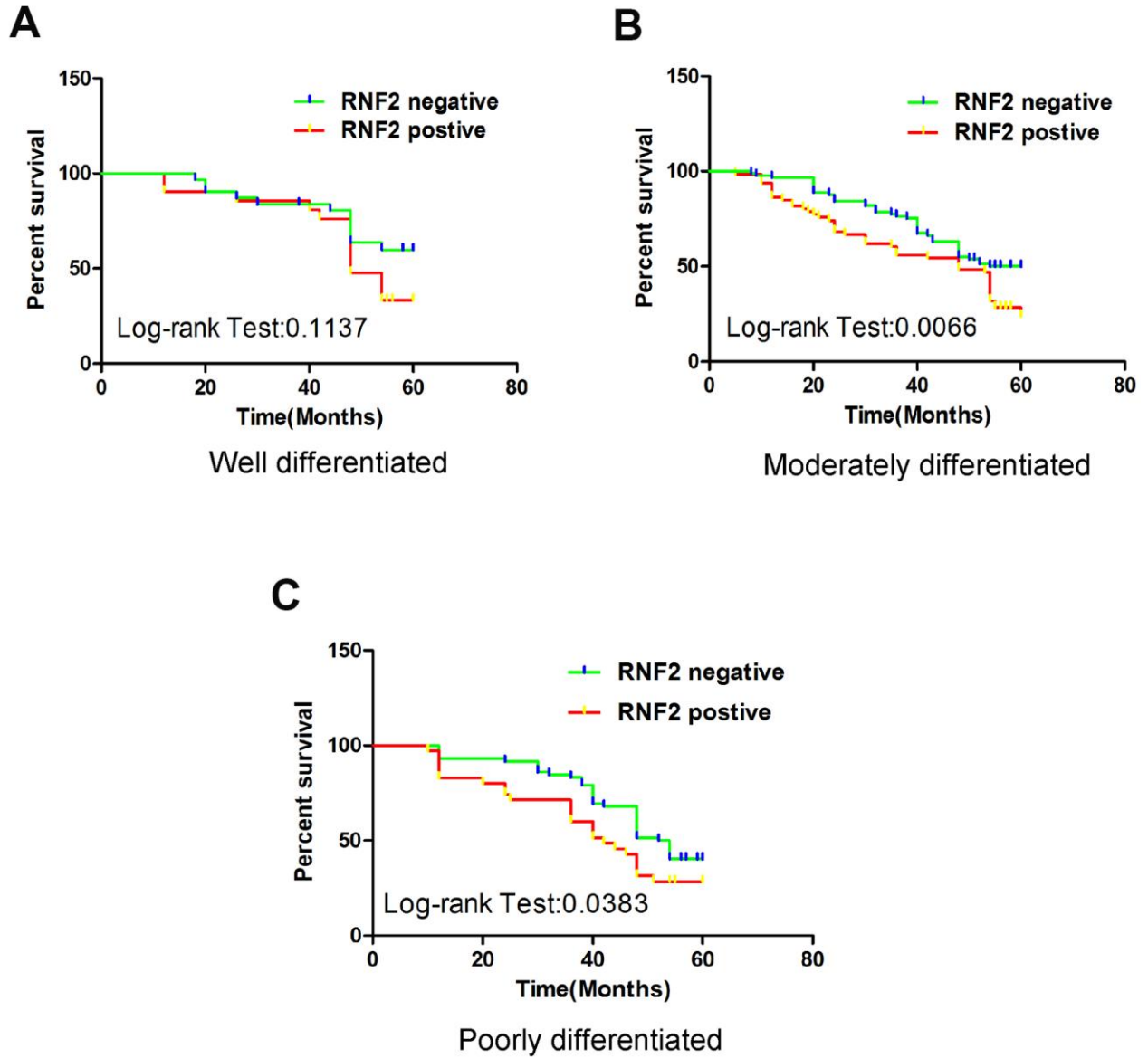
14. Schlesinger Y, Straussman R, Keshet I, Farkash S, Hecht M, Zimmerman J, Eden E, Yakhini Z, Ben-Shushan E, Reubinoff BE, Bergman Y, Simon I, Cedar H. Polycomb-mediated methylation on Lys27 of histone H3 pre-marks genes for de novo methylation in cancer. *Nat Genet.* 2007; 39:232–36.
<https://doi.org/10.1038/ng1950> PMID:[17200670](https://pubmed.ncbi.nlm.nih.gov/17200670/)
15. Schwartz YB, Pirrotta V. Polycomb silencing mechanisms and the management of genomic programmes. *Nat Rev Genet.* 2007; 8:9–22.
<https://doi.org/10.1038/nrg1981> PMID:[17173055](https://pubmed.ncbi.nlm.nih.gov/17173055/)
16. Sparmann A, van Lohuizen M. Polycomb silencers control cell fate, development and cancer. *Nat Rev Cancer.* 2006; 6:846–56.
<https://doi.org/10.1038/nrc1991> PMID:[17060944](https://pubmed.ncbi.nlm.nih.gov/17060944/)
17. Simon JA, Kingston RE. Mechanisms of polycomb gene silencing: knowns and unknowns. *Nat Rev Mol Cell Biol.* 2009; 10:697–708.
<https://doi.org/10.1038/nrm2763> PMID:[19738629](https://pubmed.ncbi.nlm.nih.gov/19738629/)
18. Lee TI, Jenner RG, Boyer LA, Guenther MG, Levine SS, Kumar RM, Chevalier B, Johnstone SE, Cole MF, Isono K, Koseki H, Fuchikami T, Abe K, et al. Control of developmental regulators by polycomb in human embryonic stem cells. *Cell.* 2006; 125:301–13.
<https://doi.org/10.1016/j.cell.2006.02.043> PMID:[16630818](https://pubmed.ncbi.nlm.nih.gov/16630818/)
19. Sánchez-Beato M, Sánchez E, González-Carrero J, Morente M, Díez A, Sánchez-Verde L, Martín MC, Cigudosa JC, Vidal M, Piris MA. Variability in the expression of polycomb proteins in different normal and tumoral tissues. A pilot study using tissue microarrays. *Mod Pathol.* 2006; 19:684–94.
<https://doi.org/10.1038/modpathol.3800577> PMID:[16528373](https://pubmed.ncbi.nlm.nih.gov/16528373/)
20. Cao L, Bombard J, Cintron K, Sheedy J, Weetall ML, Davis TW. BMI1 as a novel target for drug discovery in cancer. *J Cell Biochem.* 2011; 112:2729–41.
<https://doi.org/10.1002/jcb.23234> PMID:[21678481](https://pubmed.ncbi.nlm.nih.gov/21678481/)
21. Kim KH, Roberts CW. Targeting EZH2 in cancer. *Nat Med.* 2016; 22:128–34.
<https://doi.org/10.1038/nm.4036> PMID:[26845405](https://pubmed.ncbi.nlm.nih.gov/26845405/)
22. Li XQ, He WP, Hou WH, Chen JW, Fan RR, Yuan LJ, Yang GP, Cai MY, Chen L, Li J, He SY, Xie D, Yang GF, et al. Overexpression of RNF2 is positively associated with ovarian carcinoma aggressiveness and indicative of poor patient survival. *Oncotarget.* 2016.
<https://doi.org/10.18632/oncotarget.8975>
23. Li XD, Chen SL, Dong P, Chen JW, Wang FW, Guo SJ, Jiang LJ, Zhou FJ, Xie D, Liu ZW. Overexpression of RNF2 is an independent predictor of outcome in patients with urothelial carcinoma of the bladder undergoing radical cystectomy. *Sci Rep.* 2016; 6:20894.
<https://doi.org/10.1038/srep20894> PMID:[26869491](https://pubmed.ncbi.nlm.nih.gov/26869491/)
24. Bosch A, Panoutsopoulou K, Corominas JM, Gimeno R, Moreno-Bueno G, Martín-Caballero J, Morales S, Lobato T, Martínez-Romero C, Farias EF, Mayol X, Cano A, Hernández-Muñoz I. The polycomb group protein RING1B is overexpressed in ductal breast carcinoma and is required to sustain FAK steady state levels in breast cancer epithelial cells. *Oncotarget.* 2014; 5:2065–76.
<https://doi.org/10.18632/oncotarget.1779> PMID:[24742605](https://pubmed.ncbi.nlm.nih.gov/24742605/)
25. Wen W, Peng C, Kim MO, Ho Jeong C, Zhu F, Yao K, Zykova T, Ma W, Carper A, Langfald A, Bode AM, Dong Z. Knockdown of RNF2 induces apoptosis by regulating MDM2 and p53 stability. *Oncogene.* 2014; 33:421–28.
<https://doi.org/10.1038/nc.2012.605> PMID:[23318437](https://pubmed.ncbi.nlm.nih.gov/23318437/)
26. Su WJ, Fang JS, Cheng F, Liu C, Zhou F, Zhang J. RNF2/Ring1b negatively regulates p53 expression in selective cancer cell types to promote tumor development. *Proc Natl Acad Sci USA.* 2013; 110:1720–25.
<https://doi.org/10.1073/pnas.1211604110> PMID:[23319651](https://pubmed.ncbi.nlm.nih.gov/23319651/)
27. Koike H, Ueno Y, Naito T, Shiina T, Nakata S, Ouchi R, Obana Y, Sekine K, Zheng YW, Takebe T, Isono K, Koseki H, Taniguchi H. Ring1B promotes hepatic stem/progenitor cell expansion through simultaneous suppression of Cdkn1a and Cdkn2a in mice. *Hepatology.* 2014; 60:323–33.
<https://doi.org/10.1002/hep.27046> PMID:[24497168](https://pubmed.ncbi.nlm.nih.gov/24497168/)
28. Wei M, Jiao D, Han D, Wu J, Wei F, Zheng G, Guo Z, Xi W, Yang F, Xie P, Zhang L, Yang AG, Wang H, et al. Knockdown of RNF2 induces cell cycle arrest and apoptosis in prostate cancer cells through the upregulation of TXNIP. *Oncotarget.* 2017; 8:5323–38.
<https://doi.org/10.18632/oncotarget.14142> PMID:[28029659](https://pubmed.ncbi.nlm.nih.gov/28029659/)
29. Chen S, Chen J, Zhan Q, Zhu Y, Chen H, Deng X, Hou Z, Shen B, Chen Y, Peng C. H2AK119Ub1 and H3K27Me3 in molecular staging for survival prediction of patients with pancreatic ductal adenocarcinoma. *Oncotarget.* 2014; 5:10421–33.
<https://doi.org/10.18632/oncotarget.2126> PMID:[25431952](https://pubmed.ncbi.nlm.nih.gov/25431952/)
30. Wang W, Qin JJ, Voruganti S, Nag S, Zhou J, Zhang R. Polycomb group (PcG) proteins and human cancers: multifaceted functions and therapeutic implications. *Med Res Rev.* 2015; 35:1220–67.
<https://doi.org/10.1002/med.21358> PMID:[26227500](https://pubmed.ncbi.nlm.nih.gov/26227500/)
31. Sukhatme VP, Kartha S, Toback FG, Taub R, Hoover RG, Tsai-Morris CH. A novel early growth response gene

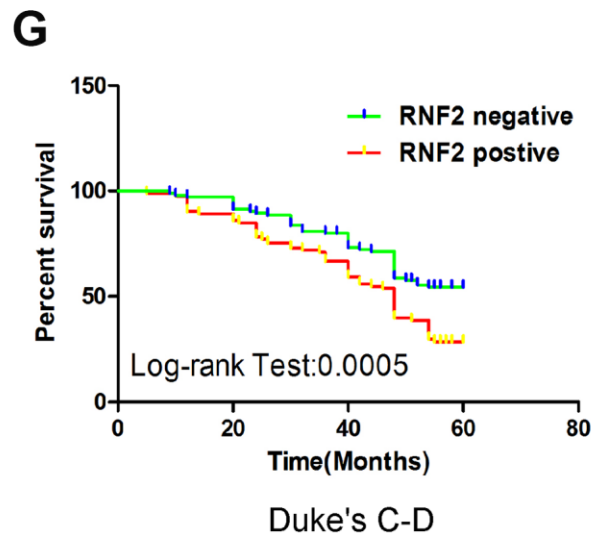
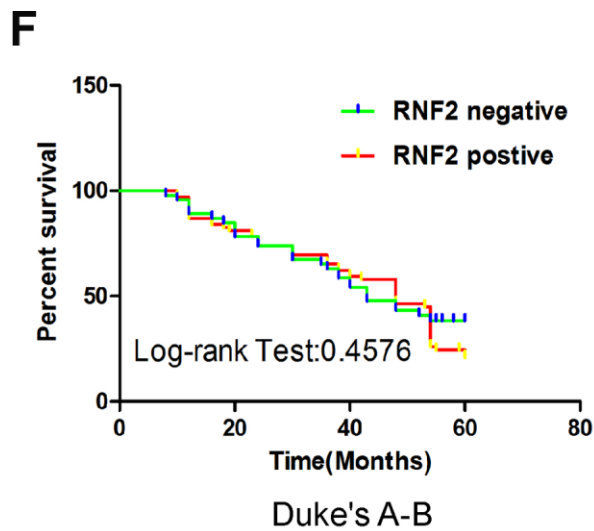
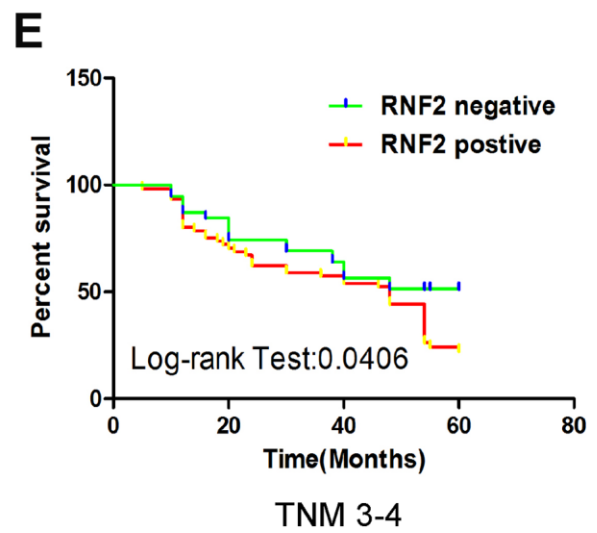
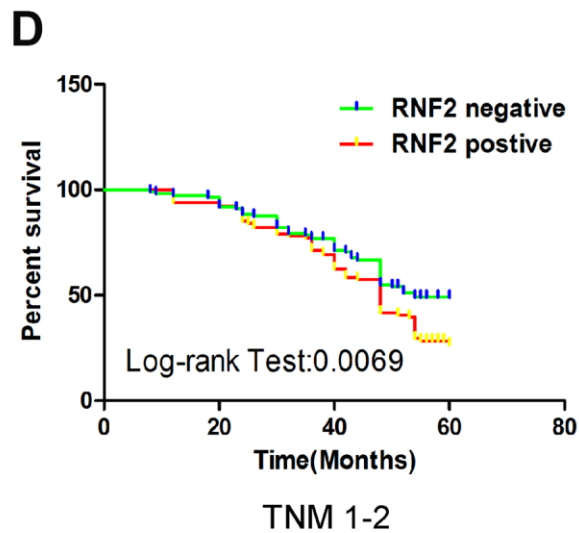
- rapidly induced by fibroblast, epithelial cell and lymphocyte mitogens. *Oncogene Res.* 1987; 1:343–55. PMID:[3130602](#)
32. Christy BA, Lau LF, Nathans D. A gene activated in mouse 3T3 cells by serum growth factors encodes a protein with “zinc finger” sequences. *Proc Natl Acad Sci USA.* 1988; 85:7857–61. <https://doi.org/10.1073/pnas.85.21.7857> PMID:[3141919](#)
33. Sukhatme VP. Early transcriptional events in cell growth: the Egr family. *J Am Soc Nephrol.* 1990; 1:859–66. PMID:[2129480](#)
34. Krones-Herzig A, Mittal S, Yule K, Liang H, English C, Urcis R, Soni T, Adamson ED, Mercola D. Early growth response 1 acts as a tumor suppressor *in vivo* and *in vitro* via regulation of p53. *Cancer Res.* 2005; 65:5133–43. <https://doi.org/10.1158/0008-5472.CAN-04-3742> PMID:[15958557](#)
35. Krones-Herzig A, Adamson E, Mercola D. Early growth response 1 protein, an upstream gatekeeper of the p53 tumor suppressor, controls replicative senescence. *Proc Natl Acad Sci USA.* 2003; 100:3233–38. <https://doi.org/10.1073/pnas.2628034100> PMID:[12629205](#)
36. Baron V, Adamson ED, Calogero A, Ragona G, Mercola D. The transcription factor Egr1 is a direct regulator of multiple tumor suppressors including TGFbeta1, PTEN, p53, and fibronectin. *Cancer Gene Ther.* 2006; 13: 115–24. <https://doi.org/10.1038/sj.cgt.7700896> PMID:[16138117](#)
37. Yu J, Baron V, Mercola D, Mustelin T, Adamson ED. A network of p73, p53 and Egr1 is required for efficient apoptosis in tumor cells. *Cell Death Differ.* 2007; 14:436–46. <https://doi.org/10.1038/sj.cdd.4402029> PMID:[16990849](#)
38. Carvalho C, L’Hôte V, Courbeyrette R, Kratassiouk G, Pinna G, Cintrat JC, Denby-Wilkes C, Derbois C, Olasso R, Deleuze JF, Mann C, Thuret JY. Glucocorticoids delay RAF-induced senescence promoted by EGR1. *J Cell Sci.* 2019; 132:jcs.230748. PMID:[31371485](#) <https://doi.org/10.1242/jcs.230748>
39. Ferraro B, Bepler G, Sharma S, Cantor A, Haura EB. EGR1 predicts PTEN and survival in patients with non-small-cell lung cancer. *J Clin Oncol.* 2005; 23:1921–26. <https://doi.org/10.1200/JCO.2005.08.127> PMID:[15774784](#)
40. Matsunoshita Y, Ijiri K, Ishidou Y, Nagano S, Yamamoto T, Nagao H, Komiya S, Setoguchi T. Suppression of osteosarcoma cell invasion by chemotherapy is mediated by urokinase plasminogen activator activity via up-regulation of EGR1. *PLoS One.* 2011; 6:e16234. <https://doi.org/10.1371/journal.pone.0016234> PMID:[21283769](#)
41. Calogero A, Arcella A, De Gregorio G, Porcellini A, Mercola D, Liu C, Lombardi V, Zani M, Giannini G, Gagliardi FM, Caruso R, Gulino A, Frati L, Ragona G. The early growth response gene EGR-1 behaves as a suppressor gene that is down-regulated independent of ARF/Mdm2 but not p53 alterations in fresh human gliomas. *Clin Cancer Res.* 2001; 7:2788–96. PMID:[11555594](#)
42. Yang M, Teng W, Qu Y, Wang H, Yuan Q. Sulforaphene inhibits triple negative breast cancer through activating tumor suppressor Egr1. *Breast Cancer Res Treat.* 2016; 158:277–86. <https://doi.org/10.1007/s10549-016-3888-7> PMID:[27377973](#)
43. Kobayashi D, Yamada M, Kamagata C, Kaneko R, Tsuji N, Nakamura M, Yagihashi A, Watanabe N. Overexpression of early growth response-1 as a metastasis-regulatory factor in gastric cancer. *Anticancer Res.* 2002; 22:3963–70. PMID:[12553019](#)
44. Cheng JC, Chang HM, Leung PC. Egr-1 mediates epidermal growth factor-induced downregulation of E-cadherin expression via slug in human ovarian cancer cells. *Oncogene.* 2013; 32:1041–49. <https://doi.org/10.1038/onc.2012.127> PMID:[22508482](#)
45. Parra E, Ortega A, Saenz L. Down-regulation of Egr-1 by siRNA inhibits growth of human prostate carcinoma cell line PC-3. *Oncol Rep.* 2009; 22:1513–18. PMID:[19885607](#)
46. Abdulkadir SA, Qu Z, Garabedian E, Song SK, Peters TJ, Svaren J, Carbone JM, Naughton CK, Catalona WJ, Ackerman JJ, Gordon JI, Humphrey PA, Milbrandt J. Impaired prostate tumorigenesis in Egr1-deficient mice. *Nat Med.* 2001; 7:101–07. <https://doi.org/10.1038/83231> PMID:[11135623](#)
47. Ozen E, Gozukizil A, Erdal E, Uren A, Bottaro DP, Atabey N. Heparin inhibits hepatocyte growth factor induced motility and invasion of hepatocellular carcinoma cells through early growth response protein 1. *PLoS One.* 2012; 7:e42717. <https://doi.org/10.1371/journal.pone.0042717> PMID:[22912725](#)
48. Kim SH, Park YY, Cho SN, Margalit O, Wang D, DuBois RN. Krüppel-like factor 12 promotes colorectal cancer growth through early growth response protein 1. *PLoS One.* 2016; 11:e0159899.

- <https://doi.org/10.1371/journal.pone.0159899>
PMID:[27442508](https://pubmed.ncbi.nlm.nih.gov/27442508/)
49. Lee SH, Bahn JH, Choi CK, Whitlock NC, English AE, Safe S, Baek SJ. ESE-1/EGR-1 pathway plays a role in tolfenamic acid-induced apoptosis in colorectal cancer cells. *Mol Cancer Ther.* 2008; 7:3739–50.
<https://doi.org/10.1158/1535-7163.MCT-08-0548>
PMID:[19074849](https://pubmed.ncbi.nlm.nih.gov/19074849/)
50. Han MH, Kim GY, Yoo YH, Choi YH. Sanguinarine induces apoptosis in human colorectal cancer HCT-116 cells through ROS-mediated Egr-1 activation and mitochondrial dysfunction. *Toxicol Lett.* 2013; 220:157–66.
<https://doi.org/10.1016/j.toxlet.2013.04.020>
PMID:[23660334](https://pubmed.ncbi.nlm.nih.gov/23660334/)
51. Choi EJ, Yoo NJ, Kim MS, An CH, Lee SH. Putative tumor suppressor genes EGR1 and BRSK1 are mutated in gastric and colorectal cancers. *Oncology.* 2016; 91:289–94.
<https://doi.org/10.1159/000450616> PMID:[27677186](https://pubmed.ncbi.nlm.nih.gov/27677186/)
52. Giraldo A, Barrett OP, Tindall MJ, Fuller SJ, Amirak E, Bhattacharya BS, Sugden PH, Clerk A. Feedback regulation by Atf3 in the endothelin-1-responsive transcriptome of cardiomyocytes: Egr1 is a principal Atf3 target. *Biochem J.* 2012; 444:343–55.
<https://doi.org/10.1042/BJ20120125>
PMID:[22390138](https://pubmed.ncbi.nlm.nih.gov/22390138/)
53. Fu L, Huang W, Jing Y, Jiang M, Zhao Y, Shi J, Huang S, Xue X, Zhang Q, Tang J, Dou L, Wang L, Nervi C, et al. AML1-ETO triggers epigenetic activation of early growth response gene 1, inducing apoptosis in t(8;21) acute myeloid leukemia. *FEBS J.* 2014; 281:1123–31.
<https://doi.org/10.1111/febs.12673>
PMID:[24314118](https://pubmed.ncbi.nlm.nih.gov/24314118/)
54. Lubieniecka JM, de Bruijn DR, Su L, van Dijk AH, Subramanian S, van de Rijn M, Poulin N, van Kessel AG, Nielsen TO. Histone deacetylase inhibitors reverse SS18-SSX-mediated polycomb silencing of the tumor suppressor early growth response 1 in synovial sarcoma. *Cancer Res.* 2008; 68:4303–10.
<https://doi.org/10.1158/0008-5472.CAN-08-0092>
PMID:[18519690](https://pubmed.ncbi.nlm.nih.gov/18519690/)
55. Su L, Cheng H, Sampaio AV, Nielsen TO, Underhill TM. EGR1 reactivation by histone deacetylase inhibitors promotes synovial sarcoma cell death through the PTEN tumor suppressor. *Oncogene.* 2010; 29:4352–61.
<https://doi.org/10.1038/onc.2010.204>
PMID:[20514024](https://pubmed.ncbi.nlm.nih.gov/20514024/)
56. Ismail IH, McDonald D, Strickfaden H, Xu Z, Hendzel MJ. A small molecule inhibitor of polycomb repressive complex 1 inhibits ubiquitin signaling at DNA double-strand breaks. *J Biol Chem.* 2013; 288:26944–54.
<https://doi.org/10.1074/jbc.M113.461699>
PMID:[23902761](https://pubmed.ncbi.nlm.nih.gov/23902761/)

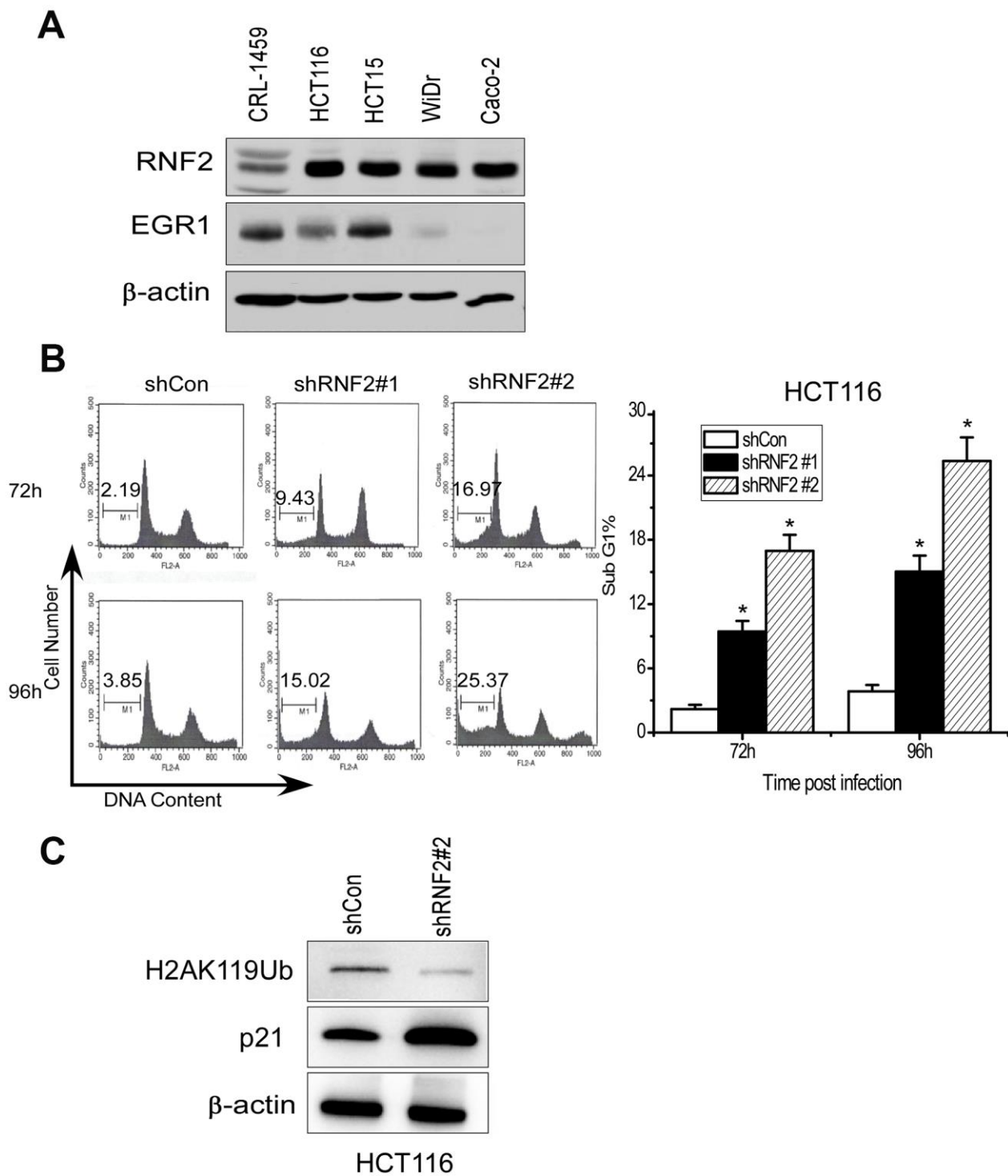
SUPPLEMENTARY MATERIALS

Supplementary Figures



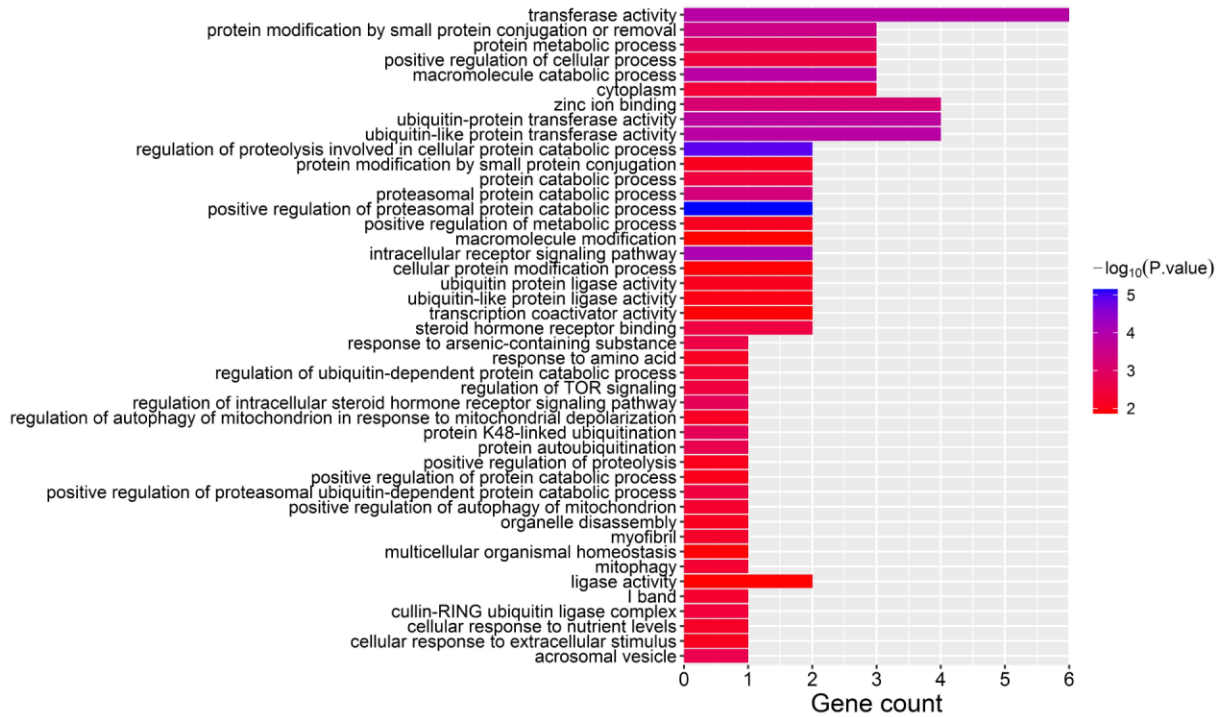


Supplementary Figure 1. The correlation between RNF2 expression and survival in patients with different differentiation status, TNM stage or Duke's stage. Patients' survival was calculated and plotted using Kaplan-Meier method. Patients were determined as RNF2 positive or RNF2 negative based on RNF2 IHC staining result. (A–C) Survival of patients with different differentiation status. In patients with moderately differentiated and poorly differentiated tumors, those had positive RNF2 expression showed worse survival. (D, E) Survival of patients in different TNM stage. In patients with tumors either in TNM 1-2 or TNM 3-4 stage, those had positive RNF2 expression showed worse survival. (F, G) Survival of patients in different Duke's stage. In patients with tumors in Duke's (C, D) stage, those had positive RNF2 expression showed worse survival.

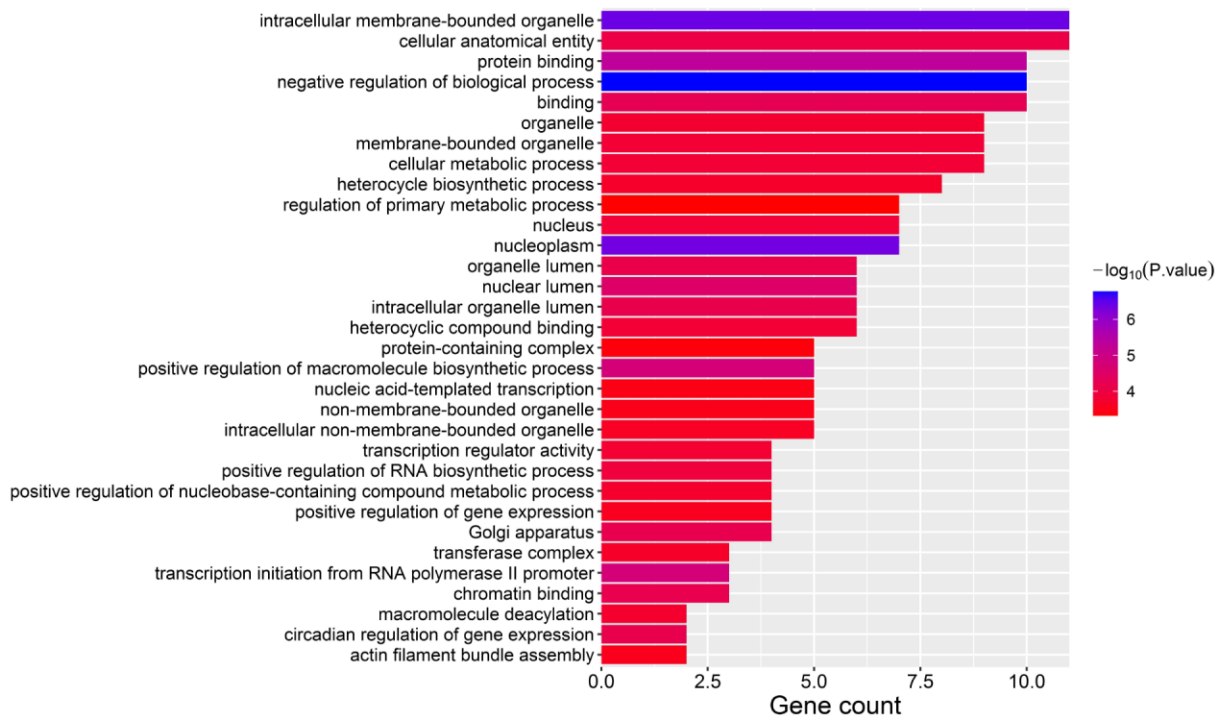


Supplementary Figure 2. Expression of RNF2 and EGR1 in CRC cells, and knockdown of RNF2 induced apoptosis in HCT116 cells. (A) Western blot analysis to show the expression of RNF2 and EGR1 in several CRC cell lines and normal colon cell CRL-1459. (B) Cell cycle analysis of control and RNF2 knockdown HCT116 cells. Data are shown as the mean \pm S.D. from three independent experiments. * p <0.05 versus shCon. (C) Western blot analysis to show the expression of p21 and H2AK119Ub in control and RNF2 knockdown HCT116 cells.

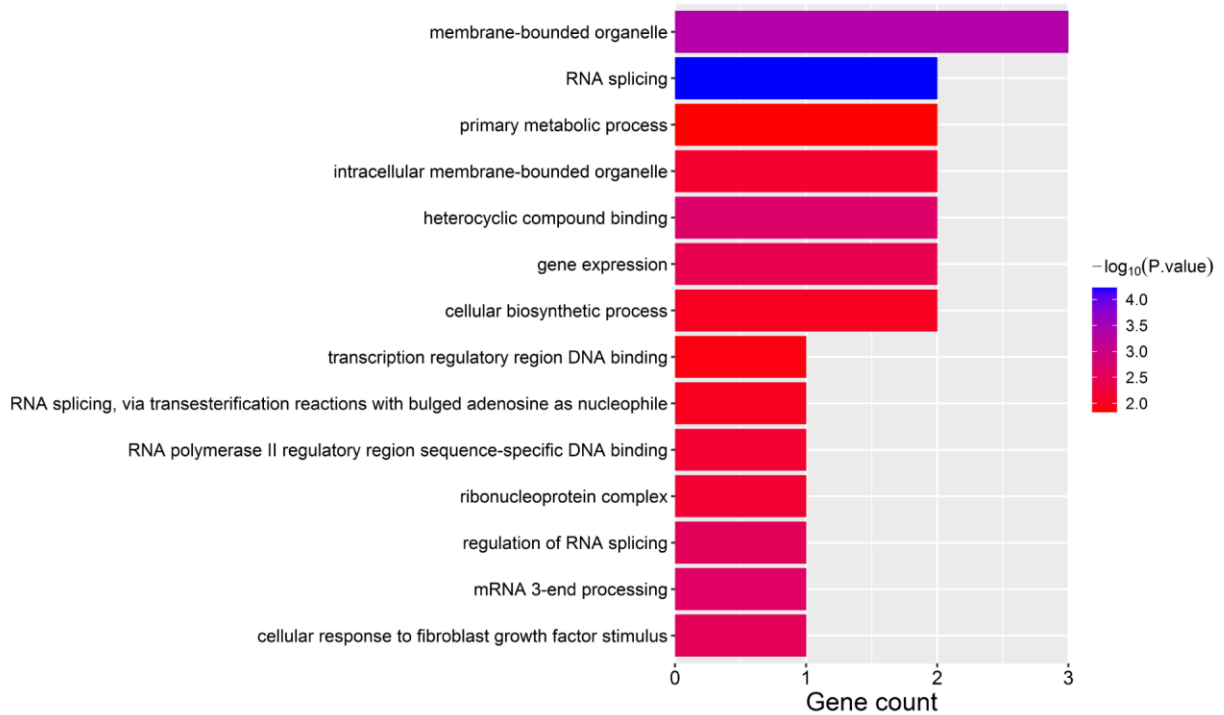
A GO enrichment analysis of the differentially expressed genes (Cluster 1)



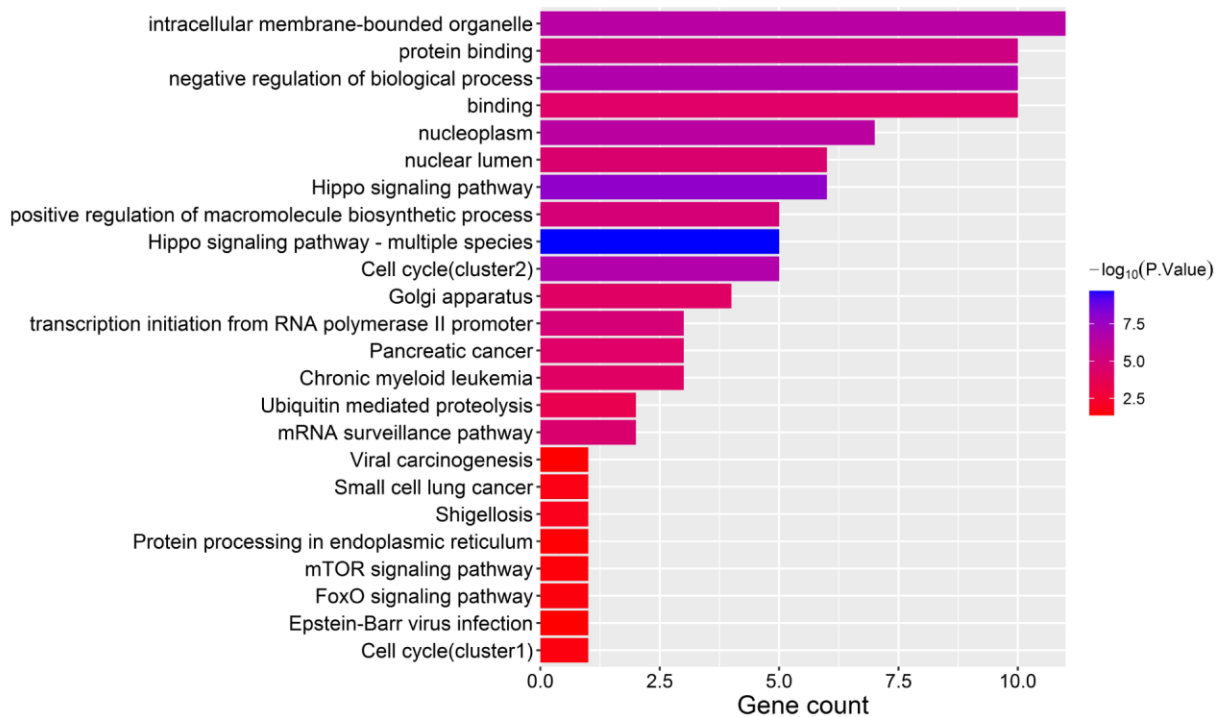
B GO enrichment analysis of the differentially expressed genes (Cluster 2)



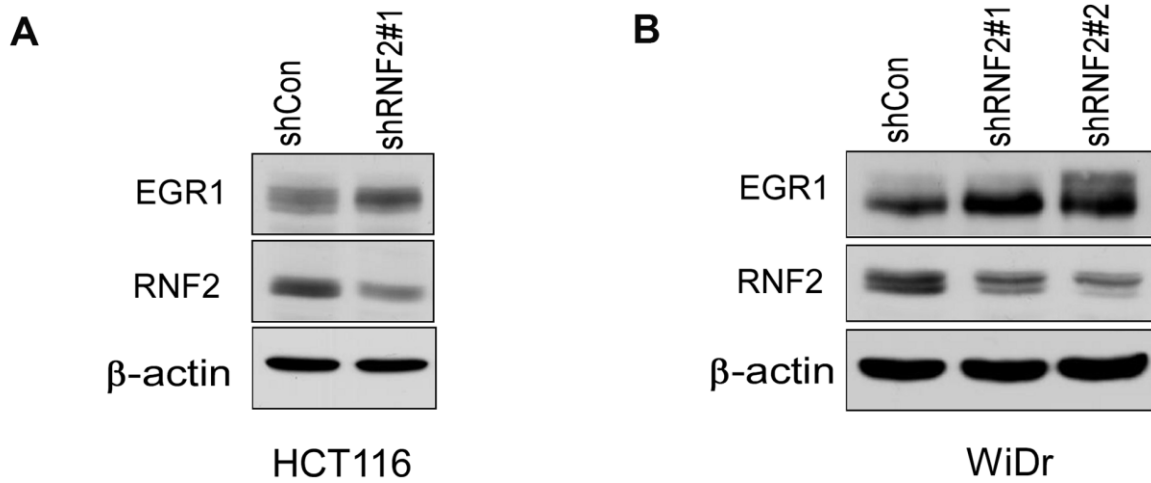
C GO enrichment analysis of the differentially expressed genes (Cluster 3)



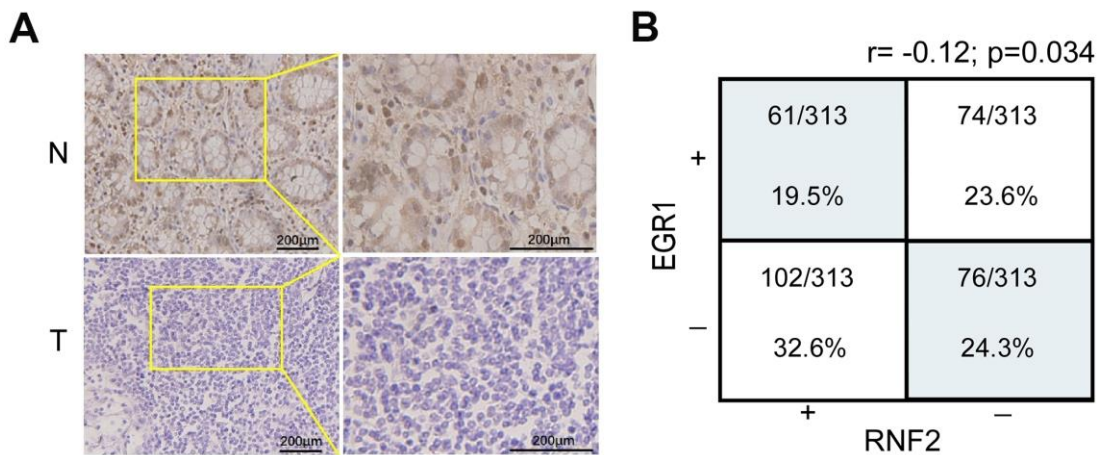
D KEGG pathway enrichment analysis of the differentially expressed genes



Supplementary Figure 3. GO biological process and KEGG pathway enrichment for the differentially expressed genes. (A–C) GO enrichment analysis of the differentially expressed genes in RNF2 knockdown cells (Cluster 1-3). The x axis indicates the number of genes within each GO term. **(D)** KEGG pathway enrichment analysis of the differentially expressed genes in RNF2 knockdown cells. The x axis indicates the number of genes within each KEGG term.



Supplementary Figure 4. Downregulation of RNF2 resulted in upregulation of EGR1 in both HCT116 and WiDr cells. (A) Western blot to show the increased EGR1 expression in RNF2 knockdown HCT116 cells (by shRNF2 #1). (B) Western blot to show the increased EGR1 expression in RNF2 knockdown WiDr cells.



Supplementary Figure 5. Correlation analysis of RNF2 and EGR1 expression in clinical CRC tissues. (A) Representative IHC staining results to show negative and positive EGR1 expression in clinical CRC tumor tissues and adjacent normal tissues. Right pictures are the magnified view of the yellow box in the left. Scale bar: 200 μ m. (B) Correlation analysis of RNF2 and EGR1 expression in clinical CRC tissues with $r = -0.12$ and $p = 0.034$.